

Identification for IPR Isomers of Fullerene C₈₂ by Theoretical ¹³C NMR Spectra Calculated by Density Functional Theory

Guangyu Sun and Miklos Kertesz*

Department of Chemistry, Georgetown University, 37th and O Streets, NW,
Washington, D.C. 20057-1227, USA

Received: December 20, 2000; In Final Form: March 19, 2001

Optimized geometries and ¹³C NMR chemical shifts of fullerene C₈₂ have been calculated by density functional theory at the B3LYP/6-31G* level for all isolated-pentagon-rule (IPR) isomers with nonvanishing HOMO-LUMO gap (isomers **1**, **2**, **3**, **4**, **5**, and **6**). The calculated ¹³C NMR spectrum of isomer **3** agrees well with the experimental spectrum of the C₂ isomer, while the predicted spectra of isomers **1** and **5** differ significantly from experiment. Thus, the observed isomer is unambiguously assigned to C₈₂:3 isomer for the first time. Both the energetic and NMR properties show that isomers **2** and **4** might be observable.

Introduction

By the means of HPLC and NMR techniques, seventeen isomers of various fullerenes have been isolated and characterized. These isomers include C₆₀,¹ C₇₀,^{1,2} one isomer of C₇₆,³ three isomers of C₇₈,^{4–6} one isomer of C₈₀,⁷ one isomer of C₈₂,⁵ and nine isomers of C₈₄.^{8–11} The isomers of fullerenes C₆₀, C₇₀, C₇₆, C₇₈, and C₈₀ have been assigned without ambiguity on the basis of the consistency between the experimentally measured NMR spectra and the NMR patterns required by point group symmetry. For the observed C₈₂ isomer, only point group symmetry can be determined⁵ as C₂ whereas the exact isomer structure cannot be assigned since three isolated-pentagon-rule (IPR) abiding isomers possess C₂ symmetry¹² and similar NMR patterns with 41 equal intensity peaks are expected for all of them. For the case of C₈₄, four of the nine isomers remain to be unambiguously assigned.¹¹ Although 2D NMR measurement would give definite answer, it is currently not a practical procedure because of the difficulty to obtain sufficient amount of sample. Experience^{13–15} has shown that density functional theory (DFT) at the B3LYP/6-31G* level is able to give accurate theoretical NMR chemical shifts for fullerenes, thus facilitate the identification of their isomers. In this paper, we address the case of fullerene C₈₂ by utilizing the DFT method, while fullerene C₈₄ will be subjected to a following study.

The electronic structures and relative stability of the nine isomers of fullerene C₈₂ have been the subject of earlier theoretical studies. All nine IPR isomers of C₈₂ are shown in Figure 1. A tight-binding molecular-dynamics (TBMD) study of C₈₂ predicted¹⁶ that isomer **3** (nomenclature after Fowler and Manolopoulos¹²) has the lowest energy and the largest HOMO-LUMO gap, while isomers **8** and **9** were predicted to distort from their ideal topological symmetry. Geometry optimizations^{17,18} carried out using the AM1 semiempirical method predicted isomer **3** to be the most stable isomer. In addition to isomers **8** and **9**, these calculations also found isomer **7** to distort from C_{3v} to C_s. Quantum consistent force field for π electrons (QCFF/PI) and PM3 calculations predicted¹⁹ that isomer **3** should have the lowest energy and second largest HOMO-

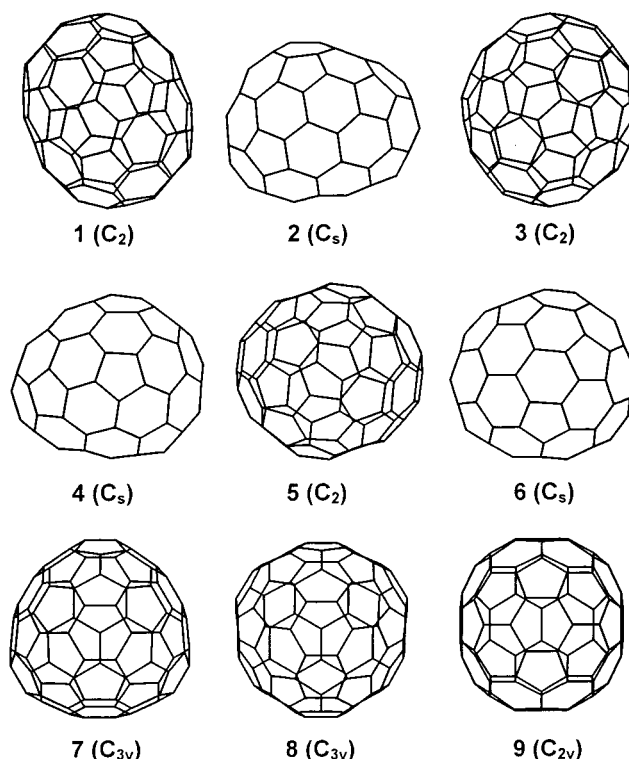


Figure 1. Nine IPR isomers of fullerene C₈₂, with topological symmetry in parentheses. Isomers are numbered according to Fowler and Manolopoulos.¹²

LUMO gap, but vibrational calculations did not show distortion for isomers **7**, **8**, and **9** at this level of theory. Local density functional (LDA) method predictions also showed isomer **3** as the most stable isomer and isomers **7**, **8**, and **9** to undergo distortion.²⁰ In a recent parallel theoretical study, DFT calculations using B3LYP/6-31G* method showed isomer **3** having the lowest energy.²¹ Thus, in general, earlier theoretical studies favor isomer **3** to have the lowest energy among the IPR isomers of fullerene C₈₂. However, experience has shown that total energy alone could not conclusively assign fullerene isomers. For instance, in the case of fullerene C₇₈, although calculations¹⁴

* Corresponding author. Phone: (202) 687-5761. Fax: (202) 687-6209. E-mail: kertesz@georgetown.edu.

TABLE 1: Bond Length Statistics and Relative Energies of IPR Isomers of Fullerene C₈₂ Calculated by Density Functional Theory^a

	C ₈₂ :1 C ₂	C ₈₂ :2 C _s	C ₈₂ :3 C ₂	C ₈₂ :4 C _s	C ₈₂ :5 C ₂	C ₈₂ :6 C _s	C ₈₂ :7 C _{3v}	C ₈₂ :8 C _{3v}	C ₈₂ :9 C _{2v}
shortest R_{cc}^b	1.365	1.363	1.371	1.369	1.366	1.367			
longest R_{cc}^b	1.470	1.472	1.470	1.472	1.471	1.473			
average R_{cc}^b	1.4328	1.4327	1.4326	1.4326	1.4326	1.4326			
B3LYP/STO-3G	7.75	6.71	0.00	5.31	10.40	15.42	<i>d</i>	38.58 ^e	23.42 ^e
B3LYP/3-21G	6.36	5.64	0.00	5.87	11.32	16.56			
B3LYP/6-31G* ^c	7.68	6.55	0.00	3.88	8.14	12.22		30.7 ^f	18.3 ^f
$\Delta E_{HOMO-LUMO}^g$	1.25	1.64	1.63	1.56	1.28	1.11			
TBMD ^h	4.40	5.21	0.00	1.75	3.83	5.28	13.05	16.86	6.57
AM1 ⁱ	4.0	6.0	0.0	6.5	12.0	16.5 ^j	31.0	35.6 ^j	21.8
PCFF/PI ^j	5.7	6.1	0.0	3.8	6.9	9.7	25.1	23.7	13.0
LDA ^k	9.6	8.9	0.0	2.8	7.2	10.8	29.7	23.6	15.1

^a Bond lengths in Å, energy in kcal/mol. ^b Bond length statistics of B3LYP/6-31G* geometries. ^c Essentially identical values were obtained in ref 21. ^d No stationary point can be located when symmetry constrained to C_{3v}. ^e First-order saddle point. ^f Taken from ref 21. ^g HOMO-LUMO gap (in eV) calculated by B3LYP/6-31G*, this work. ^h Taken from ref 16. ⁱ Taken from ref 17. ^j Taken from ref 19. ^k Taken from ref 20. ^l Taken from ref 18.

show that isomer C₇₈:3 is more stable than isomers C₇₈:1 and C₇₈:2, it is either not observed⁴ or the least abundant isomer⁶ in the extracted samples.

Theoretical predictions of NMR patterns for fullerenes have been carried out in the early days of fullerene chemistry. The chemical shifts of C₆₀ and C₇₀ with respect to benzene were predicted at the gauge-independent atomic orbital-coupled-perturbed Hartree-Fock (GIAO-CPHF) level,²² and at Hartree-Fock (HF) and density functional theory levels.²³ Calculated NMR chemical shifts of C₇₀ helped selecting the best model in interpreting the gas-phase electron diffraction (GED) experiment.²⁴ Theoretical spectral spans were used to rule out the D₂(I_h) isomer of C₈₀ as the experimentally observed isomer.⁷ The calculated spans of the NMR spectra were used to eliminate C₈₄ isomers **1** and **5** as the candidate for the observed D₂ isomer.²⁵ In recent studies by Heine et al.,^{26,27} chemical shifts of C₇₀, C₇₆, C₇₈, and C₈₄ were predicted using the individual gauge for local orbitals-density functional based tight-binding (IGLO-DFTB) method. Based on the spectral span and total energy, their results supported the assignment of the two major isomers of C₈₄. We have recently¹³ utilized the B3LYP functional in combination with the 6-31G* and 6-311G** basis sets to predict the NMR spectra of isomers **21**, **22**, and **23** of C₈₄. The small rms deviations of our predicted NMR peaks for isomers **22** and **23** allowed us for the first time to confirm solely based on NMR evidence that isomers **22** and **23** are the experimentally obtained major isomers. B3LYP/6-31G* also proved to be accurate in reproducing ¹³C NMR chemical shifts for fullerenes C₆₀, C₇₀, C₇₆, C₇₈,¹⁴ and C₈₀.¹⁵

As a part of our continued effort, the NMR spectra for the isomers of fullerene C₈₂ were studied here. All nine IPR isomers of C₈₂ are considered here. By comparing the calculated NMR spectra with the experimentally obtained spectrum, we are able to assign the observed C₂ isomer. The chemical shifts of the unobserved isomers are also presented. Energetic and NMR properties are used to compare the stability of the isomers.

Computational Method

The molecular structures of IPR isomers of fullerene C₈₂ were optimized using DFT. Becke's three-parameter (B3) hybrid functional²⁸ incorporating exact exchange in combination with Lee, Yang, and Parr's (LYP) correlation functional²⁹ was used in this study. In the first step, geometry optimizations were performed using the minimum basis set, STO-3G. To ensure that the optimized geometries were indeed minima, vibrational analyses were carried out at the B3LYP/STO-3G level of theory.

No stationary point could be located for isomer **7** when the symmetry was constrained to C_{3v}. Removing the symmetry constraint allowed it to converge to a C_s structure, confirming earlier semiempirical predictions.^{17,18} Each of isomers **8** and **9** showed one imaginary frequency at the ideal topological symmetry, which indicates that they are first-order saddle points. Earlier theoretical works showed that isomers **7**, **8**, and **9** have relative energies that are much higher than all the rest of the isomers.¹⁶⁻²⁰ Combining these facts, the three isomers (**7**, **8**, and **9**) were not included in subsequent calculations. The structure of the C₂ distorted form of isomer **9** was optimized using B3LYP/STO-3G. Since the energy of this form is only slightly lower than the C_{2v} form and the structure only slightly deviates from the C_{2v} structure, it was not further pursued. The geometries of isomers **1**, **2**, **3**, **4**, **5**, and **6** were further optimized using the 3-21G and 6-31G* basis sets.

NMR chemical shielding tensors were evaluated employing the GIAO method³⁰ at the B3LYP/6-31G* optimized geometry. The 6-31G* basis set was used upon the recommendation by Cheeseman et al.³¹ and upon our own experiences.¹³⁻¹⁵ The calculated chemical shieldings were then referenced to that of C₆₀ in order to obtain chemical shift values. The experimental chemical shift of C₆₀, 143.15 ppm, after Avent et al.,¹⁰ was used as the reference. For isomer **3**, additional geometry optimization and NMR calculation were performed at the B3LYP/6-31G level of theory. Gaussian 98³² was used for the geometry optimizations and the vibrational analyses, and the PQS suite of ab initio programs³³ was used for the NMR calculations.

Results and Discussion

Energy and Geometry. The statistics of bond lengths, HOMO-LUMO gaps calculated by B3LYP/6-31G*, and relative energies by different levels of theory are listed in Table 1 for all IPR isomers of C₈₂. The calculated molecular energy was used without zero-point energy correction. Also listed are the relative energies of C₈₂ isomers as obtained by earlier theoretical studies.¹⁶⁻²⁰ As mentioned above, no stationary point could be located for isomer **7** under C_{3v} symmetry and isomers **8** and **9** were only studied using B3LYP/STO-3G. The relative energy of the C₂ distorted form of isomer **9** was predicted to be 20.54 kcal/mol at the B3LYP/STO-3G level. Only slightly lower in energy than the ideal C_{2v} structure, the C₂ form of isomer **9** could not be the experimentally observed C₂ isomer. It is thus discarded. Similar to earlier cases,¹³⁻¹⁵ all calculated bond lengths for isomers **1-6** are within the 1.36-1.48 Å range. The

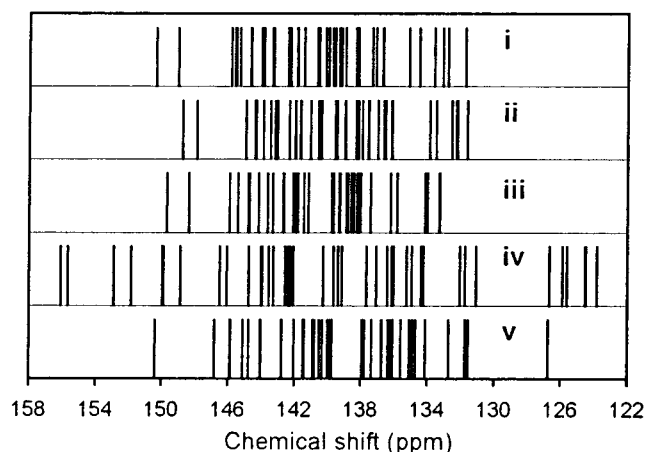


Figure 2. ^{13}C NMR spectra of C_2 isomers of fullerene C_{82} for (i) isomer **3** by experiment,⁵ (ii) isomer **3** calculated by B3LYP/6-31G, (iii) isomer **3** calculated by B3LYP/6-31G*, (iv) isomer **1** calculated by B3LYP/6-31G*, and (v) isomer **5** calculated by B3LYP/6-31G*. All spectra are referenced to C_{60} at 143.15 ppm.

average bond lengths are even more similar, varying only from 1.432 to 1.433 Å.

From the most to least stable, the order of stability of the six isomers at the B3LYP/6-31G* level is: **3** > **4** > **2** > **1** > **5** > **6**. Smaller basis sets gave comparable results on the stability. Previous theoretical results and ours are in agreement in that isomer **3** is the most stable isomer. The HOMO-LUMO gap of isomer **3** is predicted as 1.63 eV, smaller than that of isomer **2** by only 0.01 eV. The combination of the energetic and electronic properties of isomer **3** makes it the most likely isomer to be observed among the IPR isomers of C_{82} . Besides isomer **3**, isomers **2** and **4** also have relatively large HOMO-LUMO gaps and low relative energies, making their observation possible in future experiments.

NMR Chemical Shifts. Experimental NMR spectrum of fullerene C_{82} shows 41 major peaks with equal intensity and 29 peaks with moderate intensities.⁵ Thus the predominant isomer of C_{82} is one of the C_2 isomers, either **1**, **3**, or **5**, which are supposed to have 41 equal intensity peaks. The range of the 41 major peaks is 131.74–150.35 ppm, making the spectral span 18.61 ppm. Other features of the experimental spectrum include the distinct group of two peaks in the downfield region and the group of six peaks in the upfield region (see Figure 2). The rest of the 33 peaks are located in the middle part of the spectrum and are quite undistinguishable. The minor peaks were ascribed⁵ to one of the C_{3v} isomers, **7** or **8**, and the C_{2v} isomer, **9**. As we have discussed in the previous section, however, these three isomers do not have stable structures at the ideal topological symmetry, indicating that these peaks could not originate from these isomers. Another explanation of the minor peaks could be that one of the C_{3v} isomers distorts to C_3 symmetry, which should give 27 full-intensity peaks plus 1 peak with 1/3 intensity. However, repeated attempts to locate the C_3 distorted structures for isomers **7** and **8** failed, which makes us believe that the minor peaks are probably from species other than C_{82} .

Here we make a detailed comparison between theoretical and experimental NMR spectra for the C_2 isomers. As a result, the structure of the experimentally observed C_2 isomer can be assigned without ambiguity.

Table 2 lists the calculated NMR chemical shifts of isomers **1**, **2**, **3**, **4**, **5**, and **6**. The chemical shifts predicted by B3LYP/6-31G* are listed in numerically increasing order. The chemical

shifts of isomer **3** calculated by B3LYP/6-31G are listed in such a way that, for the chemical shifts in the same row, they share a common carbon atom with the chemical shifts in the B3LYP/6-31G* column. The types of carbon atoms for all isomers and the experimental chemical shifts of the C_2 isomer are also listed in Table 2. Figures 2 and 3 show the theoretical NMR spectra of the six isomers. We note that chemical shifts may have similar values and the spectrum may look like having fewer peaks than expected. In that case, the numeric values in Table 2 should give a clear view.

Let's first look at the predicted NMR spectra of the C_2 isomers, **1**, **3**, and **5**, all of which show 41 NMR peaks with equal intensity. Figure 2 shows the theoretical and experimental spectra of these isomers. The spectral spans are calculated for isomers **1**, **3**, and **5** as 32.26, 16.43, and 23.63 ppm by B3LYP/6-31G*, respectively. The experimental span of the C_2 isomer is 18.61 ppm,⁵ which is very close to calculated spectral span of isomer **3**. The calculated spectral range of isomer **3**, 133.25–149.68 ppm is also in good agreement with experimental value of the C_2 isomer, 131.74–150.35 ppm. The ranges of isomers **1** and **5** are predicted as 123.84–156.10 ppm and 126.76–150.39 ppm, respectively, differing significantly from the experimental value. This comparison clearly indicates that the observed C_2 isomer is isomer **3**.

As to the chemical shifts of individual peaks, both our calculations using the 6-31G* and 6-31G basis sets show the distinct group of two peaks in the downfield region. As noted in the earlier case¹⁵ of C_{80} , this kind of grouping of a certain number of peaks, besides the spectral span, could play a decisive role in identifying the fullerene isomers. The 6-31G* basis set fails to give correct separation between the group of six peaks in upfield region and the group in the middle part of the spectrum. This performance is in agreement with the earlier reported general trend^{13–15} where peaks above 140 ppm are better reproduced than peaks below 140 ppm when the B3LYP/6-31G* method is used. As in the earlier cases, we do not attempt one-to-one peak assignment due to the crowdedness of the peaks in the middle part of the spectrum.

The smaller basis set, 6-31G, on the other hand, successively separates the group of six peaks in the upfield region and the group in the middle part of the spectrum, thus performs equally well in both the downfield and the upfield regions. The spectral span predicted using 6-31G basis set is 17.16 ppm, which also compares better with the experimental value than the 6-31G* predicted spectral span. The 6-31G basis set previously proved to be more accurate than 6-31G* for the NMR prediction for fullerene C_{80} .¹⁵ The better performance of the 6-31G basis set as compared to the 6-31G* basis set must be due to fortuitous error cancellation. As we have shown before,^{13,15} increasing the basis set to 6-311G** does not improve the agreement between calculation and experiment. Further increasing the basis set beyond the 6-311G** basis set is not currently practical because of the size of the fullerene molecule. As such, the performance of the 6-31G basis set on the isomers C_{80} :2 and C_{82} :3 makes it a promising basis set for other higher fullerenes.

Three IPR isomers of C_{82} , **2**, **4**, and **6**, have C_s symmetry and all give 38 full-intensity peaks plus 6 half-intensity peaks. Figure 3 compiles the predicted NMR spectra for these isomers. The predicted spectra of isomers **2** and **4** have spectral spans that are normal to fullerenes. In the NMR spectrum of isomer **2**, five distinct full-intensity peaks appear in the downfield region, separated by about 1 ppm from each other. All the other full-intensity peaks appear below 146 ppm and are hard to distinguish. The six-half-intensity peaks appear at around 136.7,

TABLE 2: Theoretical and Experimental ¹³C NMR Chemical Shifts of IPR Isomers of C₈₂^a

C ₈₂ :1		C ₈₂ :2		C ₈₂ :3			C ₈₂ :4		C ₈₂ :5		C ₈₂ :6		
B3LYP/ 6-31G*	type ^b	B3LYP/ 6-31G*	type ^b	expt ^c	B3LYP/ 6-31G*	B3LYP/ 6-31G ^d	type ^b	B3LYP/ 6-31G*	type ^b	B3LYP/ 6-31G*	type ^b	B3LYP/ 6-31G*	type ^b
123.84	cor	132.82	py	131.74	133.25	131.61	py	133.28	py	126.76	cor	113.50 ^e	cor
124.50	cor	133.61	cor	132.78	133.31	133.50	cor	133.40	py	131.53	cor	115.85	cor
124.52	cor	133.99	py	133.10	134.02	132.21	py	134.22	pc	131.73	cor	120.82	cor
125.61	cor	134.67	py	133.60	134.11	132.30	py	134.75	pc	132.72	cor	122.86	cor
125.88	cor	134.92	py	134.52	134.17	132.57	py	134.79	py	132.73	cor	124.15	cor
126.67	cor	136.11	py	135.12	135.83	133.89	py	135.70	cor	134.12	py	125.76	cor
131.09	cor	136.53 ^e	py	136.68	136.23	136.14	cor	136.12	py	134.69	pc	127.27	cor
131.76	py	136.61	pc	136.71	137.42	136.99	pc	136.39	cor	134.88	cor	128.39 ^e	pc
132.06	cor	136.82 ^e	cor	137.13	138.02	138.19	pc	136.64 ^e	py	135.09	py	129.22	cor
134.24	py	137.15	pc	137.34	138.12	137.56	cor	136.80	py	135.59	cor	130.09	py
134.38	pc	137.35	py	138.18	138.23	136.51	py	136.94 ^e	cor	136.08	py	131.61	cor
134.94	cor	137.67	pc	138.27	138.43	136.64	py	136.95	cor	136.18	py	132.32	cor
135.26	py	138.62	py	138.33	138.47	136.20	py	137.17	cor	136.24	cor	132.37 ^e	pc
136.03	pc	138.68	pc	138.96	138.60	138.31	cor	137.48	cor	136.35	pc	133.05	py
136.13	py	138.85	cor	139.19	138.77	138.28	cor	138.02	pc	136.39	py	133.22	cor
136.41	py	139.02	py	139.25	138.86	137.94	cor	138.08	py	136.71	pc	133.67	cor
137.09	py	139.69	py	139.32	138.89	138.17	cor	138.11	py	136.76	cor	134.28 ^e	py
137.66	py	139.77	cor	139.58	139.25	138.93	cor	138.34	py	136.77	cor	134.88	py
139.16	cor	139.81	cor	139.72	139.33	137.58	py	139.14	py	137.35	cor	135.13	cor
139.38	py	140.10	pc	139.98	139.63	139.46	cor	139.67	cor	137.78	py	136.08	cor
139.66	cor	140.18	py	140.15	139.75	138.99	pc	140.01	pc	137.94	py	137.10	cor
140.29	py	140.24	cor	140.56	141.18	140.40	pc	140.11	py	139.74	cor	137.31	py
142.05	pc	140.67 ^e	cor	140.65	141.45	141.05	pc	140.37	cor	139.90	py	137.50	py
142.07	cor	140.93	cor	141.45	141.78	139.56	py	141.01	py	139.90	pc	138.31	py
142.27	py	141.24	pc	141.85	141.85	140.58	cor	141.19	cor	139.99	py	138.38	cor
142.38	pc	141.87 ^e	py	141.88	142.03	141.63	pc	141.21 ^e	cor	140.30	cor	138.99	pc
142.59	py	142.90	pc	142.25	142.09	141.67	cor	141.41	pc	140.52	pc	139.11	py
143.28	pc	143.64	cor	142.41	142.63	141.95	pc	142.57	pc	140.77	py	139.46	py
143.54	pc	143.82	pc	143.29	142.67	140.44	py	142.70 ^e	py	140.90	pc	139.55	py
143.92	pc	143.85	cor	143.36	142.70	141.98	pc	142.97	cor	141.39	cor	139.97 ^e	py
144.03	pc	144.15 ^e	pc	143.85	143.32	142.33	pc	143.05	cor	141.47	pc	139.98	pc
144.76	cor	144.24 ^e	pc	143.97	143.63	143.06	cor	143.23	cor	142.04	py	140.55	pc
146.08	pc	144.46	pc	144.02	144.15	143.45	pc	143.43	pc	142.77	pc	140.95	pc
146.50	pc	144.46	cor	144.65	144.16	143.18	cor	143.53	cor	144.00	cor	141.31	cor
148.88	pc	144.67	pc	144.66	144.70	144.31	cor	144.28	cor	144.04	cor	141.33	py
149.88	pc	144.82	pc	145.28	144.81	143.89	pc	144.34	cor	144.74	cor	141.56	pc
149.97	cor	144.91	pc	145.52	145.41	144.36	pc	144.91	pc	145.09	cor	142.59	cor
151.84	pc	145.77	cor	145.61	145.43	144.41	cor	144.98	pc	145.84	pc	143.38	cor
152.90	pc	146.01	pc	145.83	145.91	144.96	cor	145.73	cor	145.89	cor	143.59	pc
155.66	pc	147.06	cor	149.04	148.36	147.92	pc	147.49	pc	146.82	pc	145.97	cor
156.10	pc	148.13	cor	150.35	149.68	148.77	pc	148.59	cor	150.39	cor	147.60	pc
		150.47	cor					151.10	cor			149.42 ^e	cor
		151.73	pc					152.04 ^e	pc			150.89	cor
		152.63	pc					152.49 ^e	pc			151.77	cor

^a Chemical shifts (ppm) are calculated at the B3LYP/6-31G* optimized geometry, unless otherwise noted, and referenced to that of C₆₀ at 143.15 ppm. ^b pc, pyracylene; cor, corannulene; py, pyrene. ^c Experimental values taken from ref 5. ^d Calculated at the B3LYP/6-31G optimized geometry. ^e Half-intensity peaks.

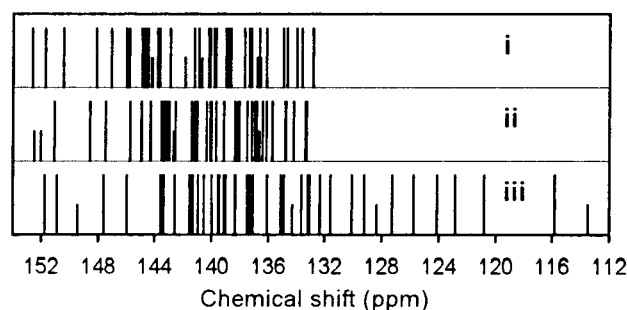


Figure 3. ¹³C NMR spectra of C_s isomers of fullerene C₈₂ calculated by B3LYP/6-31G* for (i) isomer 2, (ii) isomer 4, and (iii) isomer 6. All spectra are referenced to C₆₀ at 143.15 ppm.

141.0, and 144.2 ppm in pairs. For isomer 4, three full-intensity peaks are distinguishable in the downfield region, while the rest appear below 146 ppm. The six half-intensity peaks form three pairs, which are centered at around 136.7, 142.0, and 152.3 ppm.

The predicted NMR spectrum of isomer 6 shows a much wider spectral span than normal values for fullerenes observed so far. The lowest chemical shift is predicted at 113.50 ppm, which is far below the normal range of chemical shifts of observed fullerenes. Two groups each having 2 full-intensity peaks occur in the downfield region. One full-intensity peak appears at around 116 ppm, being separated from other full-intensity peaks by 5 ppm. The rest of the full-intensity peaks spread over the 121–144 ppm region. The half-intensity peaks also occur throughout the spectrum. Combination of the high relative energy, the low HOMO-LUMO gap and the presence of unusually low chemical shifts indicates that isomer 6 is unstable and will be difficult to observe.

Chemical Shifts and Connectivity. Three types of carbon sites were used^{3,4} to categorize the carbon atoms in fullerenes: pyracylene site (type 1, pc), corannulene site (type 2, cor), and pyrene site (type 3, py). The chemical shifts of these sites should appear in the pc > cor > py order. The type of the carbon site is given for all NMR peaks in Table 2. For the six isomers of

C₈₂, the three types appear in no particular order. Thus even within the C₈₂ isomers, local connectivity cannot be strictly correlated with chemical shifts, which is in agreement with our earlier observations.^{13–15}

In a similar study of observed isomers of fullerene C₈₄, we consider the local connectivity to further neighbors.³⁴ This scheme produces five groups of sites in the py type carbons. Each of the five groups has characteristic range of chemical shift and POAV value. Carbons of cor type and pc type can also be divided into two groups and three groups, respectively.

Conclusion

In summary, geometry optimizations have been performed for the IPR isomers of fullerene C₈₂ using density functional theory. The ¹³C NMR chemical shifts were evaluated at the B3LYP/6-31G* level of theory employing the GIAO method. The calculated ¹³C NMR spectra of isomer **3** agree with that of the experimentally observed C₂ isomer very well at both 6-31G and 6-31G* levels, providing a definite assignment of C₈₂. NMR peaks above 140 ppm are better reproduced than peaks below 140 ppm when 6-31G* basis set is used, while all peaks are predicted equally well when 6-31G basis set is used. The relatively low energies and relatively large HOMO-LUMO gaps of isomers **2** and **4** suggest that they have large energetic and kinetic stability. Their chemical shifts are also comparable to those of the observed fullerene isomers, which suggests that their observation may be possible.

Acknowledgment. This work is supported by National Science Foundation under grants CHEM-9802300 and CHEM-9601976.

References and Notes

- (1) Taylor, R.; Hare, J. P.; Abdul-Sada, A. K.; Kroto, H. W. *J. Chem. Soc. Chem. Commun.* **1990**, 1423–1425.
- (2) Johnson, R. D.; Meijer, G.; Salem, J. R.; Bethune, D. S. *J. Am. Chem. Soc.* **1991**, *113*, 3619–3621.
- (3) Ettl, R.; Chao, I.; Diederich, F.; Whetten, R. L. *Nature* **1991**, *353*, 149–153.
- (4) Diederich, F.; Whetten, R. L. *Acc. Chem. Res.* **1992**, *25*, 119–126.
- (5) Kikuchi, K.; Nakahara, N.; Wakabayashi, T.; Suzuki, S.; Shiromaru, H.; Miyake, Y.; Saito, K.; Ikemoto, I.; Kainosho, M.; Achiba, Y. *Nature* **1992**, *357*, 142–145.
- (6) Taylor, R.; Langley, G. J.; Avent, A. G.; Dennis, T. J. S.; Kroto, H. W.; Walton, D. R. M. *J. Chem. Soc., Perkin Trans. 2* **1993**, 1029–1036.
- (7) Hennrich, F. H.; Michel, R. H.; Fischer, A.; Richard-Schneider, S.; Gilb, S.; Kappes, M. M.; Fuchs, D.; Bürk, M.; Kobayashi, K.; Nagase, S. *Angew. Chem., Int. Ed. Engl.* **1996**, *35*, 1732–1734.
- (8) Dennis, T. J. S.; Kai, T.; Tomiyama, T.; Shinohara, H. *Chem. Commun.* **1998**, 619–620.
- (9) Tagmatarchis, N.; Avent, A. G.; Prassides, K.; Dennis, T. J. S.; Shinohara, H. *Chem. Commun.* **1999**, 1023–1024.
- (10) Avent, A. G.; Dubois, D.; Pénicaud, A.; Taylor, R. *J. Chem. Soc., Perkin Trans. 2* **1997**, 1907–1910.
- (11) Dennis, T. J. S.; Kai, T.; Asato, K.; Tomiyama, T.; Shinohara, H.; Yoshida, T.; Kobayashi, Y.; Ishiwatari, H.; Miyake, Y.; Kikuchi, K.; Achiba, Y. *J. Phys. Chem. A* **1999**, *103*, 8747–8752.
- (12) Fowler, P. W.; Manolopoulos, D. E. In *An Atlas of Fullerenes*; Oxford University Press: New York, 1995; pp 256–257.
- (13) Sun, G.; Kertesz, M. *New J. Chem.* **2000**, *24*, 741–743.
- (14) Sun, G.; Kertesz, M. *J. Phys. Chem. A* **2000**, *104*, 7398–7403.
- (15) Sun, G.; Kertesz, M. *Chem. Phys. Lett.* **2000**, *328*, 387–395.
- (16) Zhang, B. L.; Wang, C. Z.; Ho, K. M.; Xu, C. H.; Chan, C. T. *J. Chem. Phys.* **1993**, *98*, 3095–3102.
- (17) Nagase, S.; Kobayashi, K.; Kato, T.; Achiba, Y. *Chem. Phys. Lett.* **1993**, *201*, 475–480.
- (18) Slanina, Z.; Lee, S. L.; Kobayashi, K.; Nagase, S. *J. Mol. Struct. (THEOCHEM)* **1995**, *339*, 89–93.
- (19) Orlandi, G.; Zerbetto, F.; Fowler, P. W. *J. Phys. Chem.* **1993**, *97*, 13575–13579.
- (20) Wang, X. Q.; Wang, C. Z.; Zhang, B. L.; Ho, K. M. *Chem. Phys. Lett.* **1994**, *217*, 199–203.
- (21) Cioslowski, J.; Rao, N.; Moncrieff, D. *J. Am. Chem. Soc.* **2000**, *122*, 8265–8270.
- (22) Häser, M.; Ahlrichs, R.; Baron, H. P.; Weis, P.; Horn, H. *Theor. Chim. Acta* **1992**, *83*, 455–470.
- (23) Bühl, M.; Kaupp, M.; Malkina, O. L.; Malkin, V. G. *J. Comput. Chem.* **1999**, *20*, 91–105.
- (24) Hedberg, K.; Hedberg, L.; Bühl, M.; Bethune, D. S.; Brown, C. A.; Johnson, R. D. *J. Am. Chem. Soc.* **1997**, *119*, 5314–5320.
- (25) Schneider, U.; Richard, S.; Kappes, M. M.; Ahlrichs, R. *Chem. Phys. Lett.* **1993**, *210*, 165–169.
- (26) Heine, T.; Seifert, G.; Fowler, P. W.; Zerbetto, F. *J. Phys. Chem. A* **1999**, *103*, 8738–8746.
- (27) Heine, T.; Bühl, M.; Fowler, P. W.; Seifert, G. *Chem. Phys. Lett.* **2000**, *316*, 373–380.
- (28) Becke, A. D. *J. Chem. Phys.* **1993**, *98*, 5648–5652.
- (29) Lee, C.; Yang, W.; Parr, R. G. *Phys. Rev. B* **1988**, *37*, 785–789.
- (30) Wolinski, K.; Hinton, J. F.; Pulay, P. *J. Am. Chem. Soc.* **1990**, *112*, 8251–8260.
- (31) Cheeseman, J. R.; Trucks, G. W.; Keith, T. A.; Frisch, M. J. *J. Chem. Phys.* **1996**, *104*, 5497–5509.
- (32) Frisch, M. J.; Trucks, G. W.; Schlegel, H. B.; Scuseria, G. E.; Robb, M. A.; Cheeseman, J. R.; Zakrzewski, V. G.; Montgomery, J. A.; Stratmann, R. E.; Burant, J. C.; Dapprich, S.; Millam, J. M.; Daniels, R. E.; Kudin, K. N.; Strain, M. C.; Farkas, O.; Tomasi, J.; Barone, V.; Cossi, M.; Cammi, R.; Mennucci, B.; Pomelli, C.; Adamo, C.; Clifford, S.; Ochterski, J.; Petersson, G. A.; Ayala, P. Y.; Cui, Q.; Morokuma, K.; Malick, D. K.; Rabuck, A. D.; Raghavachari, K.; Foresman, J. B.; Cioslowski, J.; Ortiz, J. V.; Stefanov, B. B.; Liu, G.; Liashenko, A.; Piskorz, P.; Komaromi, I.; Gomperts, R.; Martin, R. L.; Fox, D. J.; Keith, T.; Al-Laham, M. A.; Peng, C. Y.; Nanayakkara, A.; Gonzalez, C.; Challacombe, M.; Gill, P. M. W.; Johnson, B.; Chen, W.; Wong, M. W.; Andres, J. L.; Gonzalez, C. M.; Head-Gordon, M.; Pople, J. A. *Gaussian 98, Revision A.5*; Gaussian, Inc.: Pittsburgh, PA, 1998.
- (33) *PQS, version 2.1*; Parallel Quantum Solutions: Fayetteville, AR, 1998.
- (34) Sun, G.; Kertesz, M. *J. Phys. Chem. A* **2001**, accepted.